The X-ray flux variations of Cygnus X-2

Bonnet-Bidaud, J.M.; van der Klis, M.B.M.

Published in:
Astronomy & Astrophysics

Astron. Astrophys. 116, 232–236 (1982)

ASTRONOMY AND ASTROPHYSICS

The X-ray Flux Variations of Cygnus X-2

J. M. Bonnet-Bidaud[1] and M. van der Klis[2,3]

[1] Section d'Astrophysique, CEN Saclay, DPh-EP/Ap, F-91191 Gif-sur-Yvette, France
[2] Astronomical Institute, University of Amsterdam, Roetersstraat 15, NL-1018 WB Amsterdam, The Netherlands
[3] Cosmic Ray Working Group, Leiden, The Netherlands

Received May 12, accepted July 20, 1982

Summary. Results of a 47 d observation of Cygnus X-2 by the COS-B X-ray experiment are presented. The observed variability of the X-ray intensity is investigated for the presence of modulation at either the $9^d.843$ optical period or the $11^d.23$ X-ray period claimed for this source. Upper limits are given to pulse amplitudes for periods between 1 d and 200 s.

Clear dips were observed during the time of highest source intensity, with transitions of up to 40% in the source flux in less than $1–2\,10^3$ s. It is suggested that the dips may be connected to the reported UV flaring activity.

Key words: X-ray sources – Cygnus X-2 – COS-B

Introduction

The X-ray source Cyg X-2 was associated, at an early time, with the variable star V 1341 Cyg (Giacconi et al., 1967). Extensive search for periodicities from optical photometry has lead to the proposal of periods ranging from 0.9 to 14 d (Chevalier et al., 1976; Wright et al., 1976; Basko, 1977), while a convincing $9^d.8$ orbital period was more recently determined on the basis of optical line velocities (Cowley et al., 1979).

The X-ray source is found to vary between a typical low and high state. The presence of a $9^d.8$ X-ray modulation was claimed in low state (Marshall and Watson, 1979; Ilovaisky et al., 1979), but was not confirmed from long baseline observations which seem to indicate an $11^d.2$ period instead (Holt et al., 1979). The nature of the source is still a matter of strong debate with two contradictory models, one involving a degenerate dwarf at 250 pc (Branduardi et al., 1980), the other a neutron star at 8 kpc (Cowley et al., 1979).

Previously published X-ray observations were made with a relatively sparse daily coverage (Parsignault and Grindlay, 1978; Holt et al., 1979; Branduardi et al., 1980). We report here on a 47 d COS-B X-ray observation of the source with continuous 100 s resolution coverage of the source flux over periods of 30 h.

Observations

The COS-B X-ray detector is an 80 cm^2 collimated proportional counter with an energy range of 2–12 keV (see Boella et al., 1974). Cygnus X-2 was in the 10° FWHM field of view of this detector permanently between June 2nd and July 19th, 1981; it was observed at a geometrical efficiency of 0.6. SS Cyg (4U2140+33) was also in the detector field at an efficiency of somewhat less than 0.5; at maximum intensity (Bradt et al., 1979) it would have contributed about 1 c/s to the total counting rate.

Due to the high apogee (10^5 km) of the orbit of the COS-B satellite, the X-ray experiment is characterized by a high charged particle background. Most of this background is eliminated on-board by anti-coincidence and pulse-shape discrimination. The residual background is subtracted by means of its relation to the near-simultaneously measured charged particle rate, as known from pointings to fields empty of detectable X-ray sources. This relation is usually reproducible to ~1 c/s from one observation to another but we cannot exclude systematic effects due to changes in the mean properties of the charged particles within one observation. During the observation of Cygnus X-2, the charged particle background varied between 55–65 c/s on a typical time scale of 10 d. After the background subtraction and correction for aspect, the resulting X-ray counting rate, shown in Fig. 1, is in the 20–50 c/s bracket. This corresponds to a flux of 5.2 to $13\,10^{-9}$ erg cm^{-2} s^{-1} (2–12 keV) for an assumed 5 keV bremsstrahlung spectrum (Branduardi et al., 1980), consistent with a low to moderate intensity level of Cyg X-2 (Bradt et al., 1979).

The data gaps in Fig. 1 are the result of periodic satellite switch-off upon entry of the radiation belts (once every 36 h) and rejection of data because of occasional charged particle storms. Each 2048 s bin corresponds to the average of 20 equally spaced $25^s.6$ measurements, statistical error per bin is about 0.7 c/s. The signal is variable on all time scales from 10 d (not correlated to the background variability) down to the 100 s temporal resolution of the data. Sudden transitions in the intensity of up to 40% and numerous dips of similar depth, all uncorrelated to the particle background, are visible throughout the observation, superposed to a smoother flux variation.

Analysis and Results

Period Search

The data have been investigated for periodic intensity modulations using both folding and FFT techniques. Possible modulations at the $11^d.23$ ASM X-ray period (Holt et al., 1979) and the $9^d.843$ spectroscopic optical period (Cowley et al., 1979) could not have been discovered from the present 47 d observation. To test whether a modulation at either of these periods can be found back

Send offprint requests to: J. M. Bonnet-Bidaud

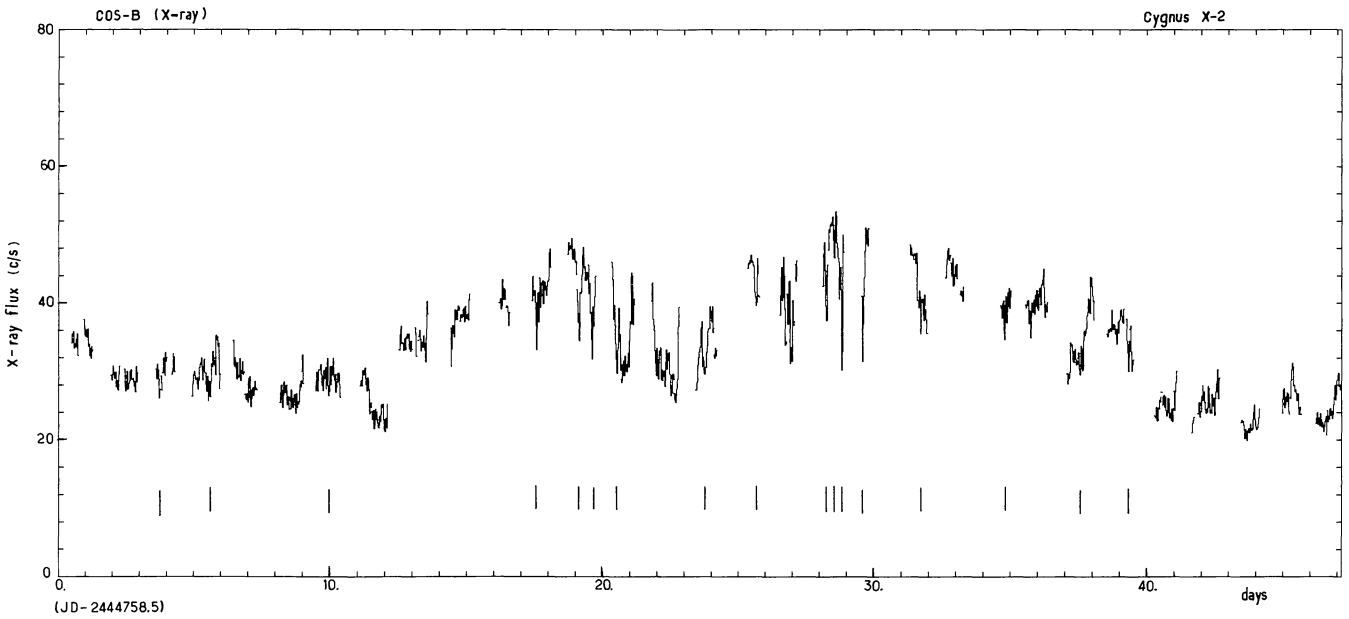

Fig. 1. The counting rate from Cygnus X-2 after background subtraction and aspect correction. Statistical error on each 34 min bin is about 0.7 c/s. Strong dips are visible and marked by vertical lines (see also Table 2)

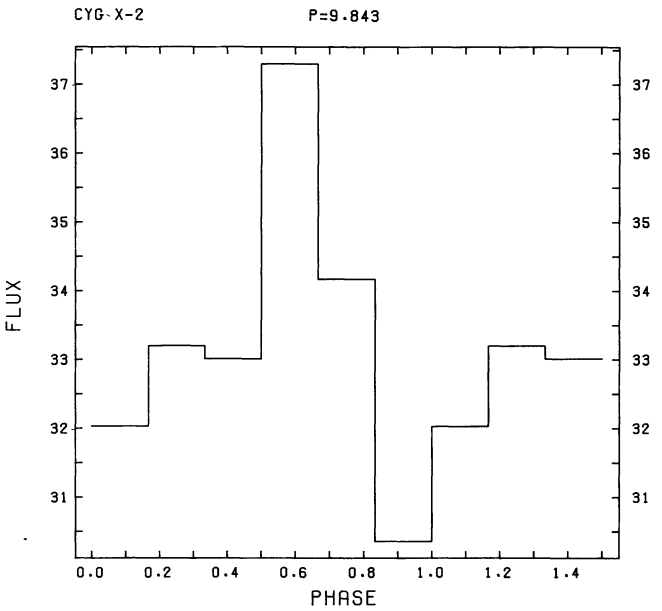

Fig. 2a. The Cygnus X-2 counting rate folded using the predicted X-ray ephemeris of Cowley et al. (1979) with a period of $9^d.843$. Formal error per bin is less than 0.5 c/s

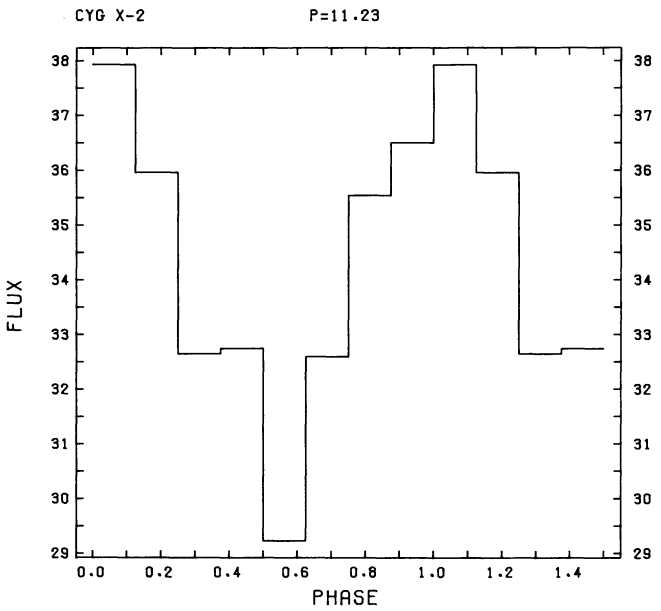

Fig. 2b. Same as **a**, with the folding period of $11^d.23$ from the ephemeris of Holt et al. (1979)

in the observed X-ray variability, the signal was folded according to the corresponding ephemerides: $T = \text{JD } 2443000.9 + 11.23\,E$ and $T = \text{JD } 2443166.7 + 9.843\,E$ (predicted X-ray phase). The resulting light curves are given in Fig. 2. It should be kept in mind, that these light curves could be spurious, resulting from irregular flux variations. Indeed, the charged particle background, when folded, shows "light curves" of similar modulation depth (but of different shape and phase) as the X-ray flux.

The $11^d.23$ light curve resembles the "sawtooth" shaped one seen in the ASM data, with the maximum occurring about 0.06 (ASM: 0.07) later in phase than midway between the minima, and a best fit sinusoidal amplitude of 9.0% (ASM: 7.2%). The epoch of the minimum of the best-fit sine wave is JD 2444780.6 ± 0.6, halfway between the predicted minima. This corresponds to a correction to the $11^d.23$ period of plus or minus $0.03 \pm 0^d.01$, consistent with the $0^d.03$ error quoted by Holt et al. (1979). The trace resulting from the $9^d.843$ folding has its minimum at JD 2444780.1 ± 0.8 close to the value of JD 2444781.0 ± 0.4 predicted for the X-ray star superior conjunction (Cowley et al., 1979). The relative full amplitude from a sine fit to the modulation

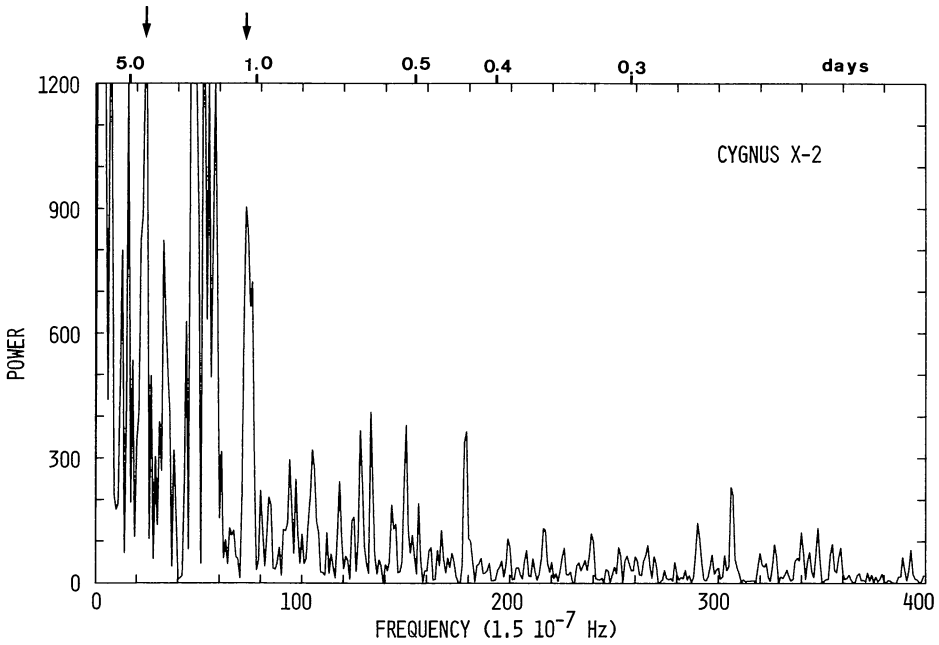

Fig. 3. The Cygnus X-2 power spectrum. The low frequency part of the spectrum is shown, with the power normalized to 1 in the high frequency part. The complex structure around $1^d.5$ ($n \sim 50$) corresponds to the satellite orbital period. Peaks at $1^d.06$ ($n \sim 73$) and $3^d.2$ ($n \sim 24$) (marked by arrows) are not found in the background transform

Table 1. Upper limits for coherent pulsations in Cygnus X-2

Period range	Highest relative semi-amplitude
1.1 −0.26 d	4 %
0.26 −0.19 d	2 %
0.19 −0.065 d	0.8 %
0.065 −0.035 d	0.5 %
0.035 d − 200 s	0.2 %

is 14%, much lower than the 35–40% reported by Ilovaisky et al., (1979). The light curve is also visible in the higher luminosity part of the observation (days 12–40 in Fig. 1) only.

In conclusion, the observed shape and amplitude of the $9^d.843$ and $11^d.23$ period light curves do not favour either of these periods above the other, though the phase coincidence with the ephemeris for the $9^d.843$ period, predicted from optical line velocities (Cowley et al., 1979), is better.

For further period searching, we constructed a 2^{16} bin power spectrum of the signal with a resolution of $1.5\,10^{-7}$ Hz. Figure 3

Table 2. Characteristics of the Cygnus X-2 dips

Date (JD 2444000.0)	Source int. (c/s)	Dip rel. ampl. (%)	Dip width FWHM (h)	Trans. time (h)	Phase[a] (9.8 d)	(11.23 d)
762.23	28.5	18.6	0.25	0.14	0.61	0.84
764.31	32.8	19.5	0.48	0.21	0.82	0.03
768.47	27.7	16.9	0.27	0.14	0.24	0.40
776.07	40.2	18.6	1.21	0.21	0.01	0.07
777.65	47.2	20.3	3.12	1.70	0.17	0.21
778.10	42.3	22.7	2.88	1.80	0.22	0.26
779.02	38.1	22.3	2.16	1.30	0.31	0.59
782.25	37.0	22.9	4.32	2.72	0.64	0.62
784.17	44.7	14.3	0.96	0.42	0.84	0.80
785.33	41.7	21.8	0.48	0.28	0.95	0.90
785.47	41.9	30.5	1.92	0.42	0.97	0.91
786.76	49.8	23.9	2.16	0.71	0.10	0.03
787.05	52.8	16.7	0.72	0.35	0.13	0.05
787.33	48.9	39.2	1.20	0.56	0.16	0.08
788.10	43.2	27.1	1.97	0.71	0.24	0.15
790.20	40.2	13.2	0.51	0.21	0.45	0.33
793.30	38.9	13.6	1.22	0.21	0.76	0.61
796.16	33.6	12.5	0.89	0.35	0.06	0.86
797.82	35.1	15.1	1.23	0.85	0.22	0.01

[a] Phases are computed according to the following ephemerides:
Spectroscopic phase: $T = 2443161.68 + 9.843\,E$ (Cowley et al., 1979) (spectroscopic phase, corresponding to X-ray phase 0.52);
X-ray phase: $T = 2443000.9 + 11.23\,E$ (Holt et al., 1979)

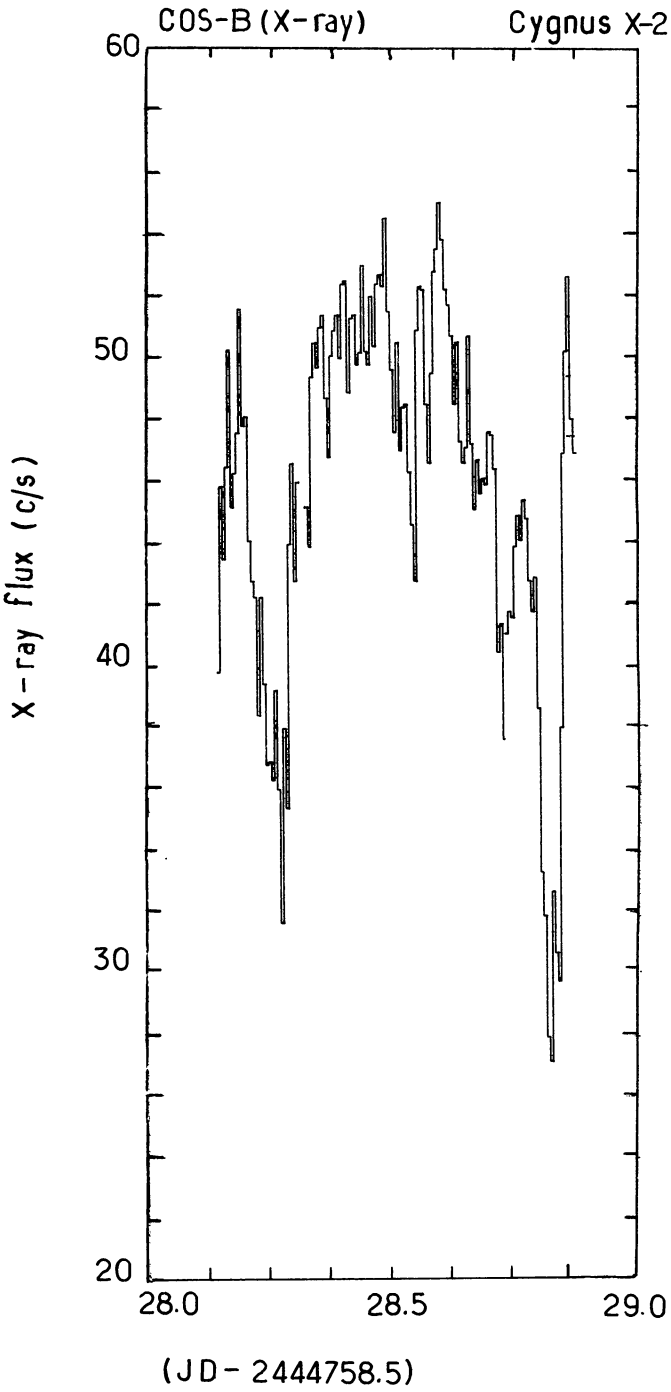

Fig. 4. Detailed structure of some of the source dips. Each bin is 8.5 min duration with typical error bar of about 1 c/s. Notice the rapid transitions ($\sim 10^3$ s) even for the deepest dip

shows the low frequency region of this power spectrum; the power was normalized to a mean value of 1 in the high frequencies. The highest power (apart from the low frequency noise) is attained in the complex structure around $1^d.5$. This feature corresponds to the $1^d.53$ satellite orbital period; it is also present in the transform of the charged particle background. The peaks at $3^d.2$ and $1^d.06$ might just be significant; they have no clear counterparts in the background transform, but could easily be the result of a combination of irregular fluctuations and window effects (notice also the approximate 1:2:3 ratio of the frequencies involved).

For shorter periods, the power spectrum allows us to put upper limits to the relative amplitude of coherent pulsations from Cyg X-2. The theoretical statistical 99% confidence detection level limit can be calculated for this case as 0.1%; intrinsic source fluctuations increase this value appreciably, especially towards lower frequencies. Table 1 lists the highest detected power, expressed in terms of relative semi-amplitude of the corresponding modulation, for several frequency regions.

In practice, due to Doppler shifts, the power of a pulsating X-ray source in an orbit with $a_x \sin i = 5\,10^{11}$ cm and $P_{orb} = 9^d.843$ (Cowley et al., 1979) will be spread out over about $1700\,\mathrm{s}/P_{puls}$ bins in the power spectrum. For the shortest detectable periods ($P_{puls} = 200$ s), this effect increases the detection limit by a factor of about 3.

The absence of detectable pulsations is in line with the general Population II X-ray source character of Cyg X-2 (no eclipses, soft spectrum, high L_x/L_{opt}); see, e.g., Parsignault and Grindlay (1978).

Dips in the Cyg X-2 *Flux*

Ilovaisky et al. (1979) reported the occurrence of X-ray dips and a deep (14 h duration) minimum at X-ray phase 0.5. In the present data, similar but slightly less deep minima are visible at various phases (see at JD 2444770.0, 79.0, and 80.0 in Fig. 1). The nearly continuous recording of the X-ray flux with the COS-B experiment allows the study of flux variations as short as a few minutes (no spectral information is available).

A set of 19 clear dips (duration less than $0^d.5$) in the X-ray intensity was selected and studied in a detailed way (see Table 2). Most of the dips (12) occur between JD 2444775.0 and JD 2444789.0, during the time of highest source intensity (see Fig. 1).

They are variable in strength and shape with relative amplitudes ranging from 12 to 40%, half-maximum widths from 15 min to 4 h and transition times from 8 min to 2 h.

A few of these transitions are shown in more detail in Fig. 4. Even for the deepest dips, the intensity can drop or recover very quickly, within $1\text{–}2\,10^3$ s (compare Ilovaisky et al., 1979).

We have looked for regularity in the occurrence of the dips with respect to the periods of $9^d.8$ and $11^d.23$ claimed for the source. The phases of the dips are indicated in Table 2. We note that the strongest dips occur predominantly in a (0.0–0.3) phase interval of the $9^d.8$ period, with all but one being in the (0.6–0.3) interval (phase 0.0 corresponding to the optical star superior conjunction, or X-ray phase 0.52). However the restricted sample does not clearly establish this effect; in particular, as the two proposed periods are nearly in phase during the observing period, a similar but less impressive clustering is also observed for the $11^d.23$ period. The optical star, V 1341 Cyg, exhibits erratic variations on timescales of minutes of several tenths of a magnitude (Kristian et al., 1967), which can be interpreted as UV flaring activity, preferentially occurring in the same $9^d.8$ phase interval 0.6–0.3 (Cowley et al., 1979). If the clustering of the X-ray dips is real, this would relate the two phenomena. Since $L_x/L_{opt} \sim 100\text{–}450$ (Bradt et al., 1979), this suggests that the X-ray flux during the dips may be reprocessed into UV with an efficiency of the order of a percent. Simultaneous observations are indicated to check for time coincidence of these events.

Acknowledgements. The authors thank J. van Paradijs for reading the manuscript. M. vdK acknowledges financial support by the

Netherlands Organisation for the Advancement of Pure Research Z.W.O. (Astron).

References

Basko, M.M.: 1977, *Ann. NY Acad. Sci.* **302**, 403
Boella, G., Buccheri, R., Burger, J., Coffaro, P., Paul, J.: 1974, Proc. 9th ESLAB Symp., ESRO SP-106, 345
Bradt, M., Doxsey, R., Jernigan, J.: 1979, *Adv. Sp. Epl.*, Vol. 3
Branduardi, G., Kylafis, N.D., Lamb, D.Q., Mason, K.O.: 1980, *Astrophys. J. Letters* **235**, L153
Chevalier, C., Bonazzola, S., Ilovaisky, S.A.: 1976, *Astron. Astrophys.* **53**, 313
Cowley, A.P., Crampton, D., Hutchings, J.B.: 1979, *Astrophys. J.* **231**, 539
Giacconi, R., Gorenstein, P., Gursky, H.H., Usher, P., Waters, J., Sandage, A., Osmer, P., Jugaku, J.: 1967, *Astrophys. J. Letters* **148**, L129
Holt, S.S., Kaluzienski, L.J., Boldt, E.A., Serlemitsos, P.J.: 1979, *Astrophys. J.* **233**, 344
Ilovaisky, S.A., Chevalier, C., Motch, C., Janot-Pacheco, E.: 1979, IAU *Circ.* 3325
Kristian, J., Sandage, A., Westphal, J.A.: 1967, *Astrophys. J. Letters* **150**, L183
Marshall, N., Watson, M.G.: 1979, IAU *Circ.* 3318
Parsignault, D.R., Grindlay, J.E.: 1978, *Astrophys. J.* **225**, 970
Wright, E.L., Gottlieb, E.W., Liller, W., Grindlay, J., Schnopper, H., Schreier, E., Gursky, H., Parsignault, D.: 1976, *Bull. Amer. Astron. Soc.* **8**, 441